



# Experimental study of the critical flashing flow through a relief line: evidence of the double-choked flow phenomenon

A. Attou\*, L. Bolle, J.M. Seynhaeve

*Unité de Thermodynamique et Turbomachines, Université catholique de Louvain 2, Place du Levant, 1348 Louvain-la-Neuve, Belgium*

Received 17 June 1998; received in revised form 24 June 1999

---

## Abstract

New experimental results are presented for steady-state critical steam–water flows through a horizontal relief line involving an abrupt cross-sectional area change. In the stagnation conditions, the pressure is fixed to 6 bars and the temperature is varied in the range of 110–150°C. Two geometrical singularities are tested: the sudden enlargement and the circular orifice. For both geometrical configurations, the occurrence of the so-called double-choked flow phenomenon is demonstrated on the basis of experiments performed by varying the back-pressure. For a small enough value of the back-pressure, two simultaneous stable locations of critical sections are highlighted: the first one is located close to the singularity and the other is located at the outlet of the relief line. The maximum possible value of the mass flowrate is limited only by the first critical section. The occurrence of the second critical section does not affect the mass flowrate any more. The interpretations of the associated transfer phenomena (the locations of critical sections, the critical mass flowrate and pressure ratio) are supported by the visualisation of three stable flashing flow patterns close to the singularity: the confined free jet, expanded jet and submerged jet patterns. © 2000 Elsevier Science Ltd. All rights reserved.

*Keywords:* Flashing flow; Double-choked flow; Critical mass flowrate; Sudden enlargement; Orifice; Pressure relief line; Back-pressure; Jet patterns; Thermal non-equilibrium

---

---

\* Corresponding author. CMI-Defense, Voie de l'Ardenne 134, BE 4053, Embourg, Belgium..

*E-mail address:* abdel.attou@cmi.be (A. Attou).

## 1. Introduction and literature survey

The relief lines located downstream from safety devices (safety valves and rupture disks for example), installed for protecting pressurized vessels or reactors, involve several geometrical singularities such as abrupt area changes (sudden enlargement, sudden contraction or orifice) and abrupt direction changes (elbows or tee junction). The sudden enlargement and the orifice are two examples of abrupt cross-sectional area changes which are of a great importance in the industrial practice. Indeed, the abrupt enlargement is often encountered in pressure relief lines of chemical and petroleum engineering processes. Furthermore, several geometrical singularities (valve, sudden contraction, constriction, etc.), which exhibit a local hydrodynamic resistance, can be approximately represented by an equivalent orifice.

During a discharge operation, the hydrodynamic parameters influencing the protection of the pressurized vessel or reactor are the mass flowrate and the pressure ratio. These ones are often critical due to the high value of the pressure difference between the upstream vessel and the catch tank. The critical mass flowrate is strongly reduced by the vaporisation phenomenon and significantly depends on the location of the critical section (Bolle et al., 1995). The prediction of this location is a difficult problem due to the complexity of the relief line geometry. Furthermore, the occurrence of multiple simultaneous locations of critical sections can prevail in the choked flow through a pressure relief line involving several abrupt area changes (Attou et al., 1996). In these conditions, perturbations of the safety device operation can be observed. An analysis of the published works concerning this topic shows that this phenomenon of simultaneous appearance of several critical sections, the so-called multiple choked flow phenomenon, is almost not analysed in the literature. The essential objective of this study is to highlight experimentally the existence of the multiple choked flow and to present a phenomenological analysis of the associated phenomena (jet flow patterns, critical mass flowrate and pressure ratio).

A significant part of the published studies of two-phase flow (either with or without flashing) through abrupt area changes have been performed in subcritical regime (Delhaye, 1981; Tapucu et al., 1989; Schmidt and Friedel, 1997). In these conditions, the averaged flow velocity is small compared to the local velocity of sound and the compressibility effects are negligible. The important hydrodynamic parameter for design purposes is the pressure loss. The major part of the published models for pressure loss of two-phase subcritical flows through an abrupt cross-sectional area change can be summarized by a general approach based on the macroscopic balance equations.

Experimental studies of critical two-phase flows through orifices and short tubes have been performed by some authors (Zaloudek, 1963; Ogasawara, 1969a) in order to develop correlations for the critical mass flowrate. Zaloudek (1963), Henry (1970) and Henry and Fauske (1971) have shown that the critical discharge mass flowrate is affected by the geometry of the pipe, the entrance effects and the ratio of the pipe length over the diameter ( $L/D$ ). The influence of the geometrical parameter  $L/D$  has been also observed by Fauske (1965). This author has concluded that when the ratio  $L/D$  increases the critical mass flowrate comes closer to the value predicted from the model based on the thermodynamic equilibrium of phases. On the basis of experimental results related to the void fraction, Seynhaeve (1977) has shown that the critical flow of initially subcooled water vaporising across an orifice has a structure similar

to that reported by the above researchers in the case of short tubes ( $0 < L/D < 3$ ): a central water jet surrounded with vapour. The critical discharge of superheated liquid from pressurized vessel and pipes have been analysed experimentally by Fletcher and Johnson (1983) and Van den Akker and Bond (1984). Comprehensive reviews of theoretical and experimental work related to critical two-phase flows can be found in the references of Giot (1981), Hsu and Graham (1986) and Alimonti (1996).

It can be concluded that previous studies are only focused on the geometrical singularity itself or the pipe itself but not on the global problem of a two-phase choked flow through a whole discharge line involving, among others, abrupt cross-sectional area changes. However, the analysis of this problem is of great importance in the industrial practice for design and operation of safety relief systems (Morris, 1990). In our knowledge, not any existing work in the literature has been dedicated to a systematic analysis of the phenomenon of simultaneous location of multiple critical sections (the so-called multiple choked flow) since this phenomenon is a characteristic of the whole pipe system.

The aim of this study is to present original experimental results over steady-state flashing water flow through a discharge line which involves one geometrical singularity: an abrupt enlargement or an orifice. The experimental evidence of critical conditions and the double-choked flow phenomenon (two simultaneous locations of critical sections) as well as the associated phenomenology (jet patterns, location of critical sections, critical mass flowrate and pressure ratio) are discussed.

## 2. Experimental facility

The scheme of the experimental loop is given in Fig. 1. A detailed description of this loop is presented by Attou (1997). The upstream vessel is filled with hot pressurized water. Water is heated to the required temperature (stagnation temperature  $T_0$  between 110 and 150°C) by circulating through the boiler. The circuit linking the boiler to the upstream vessel is interrupted during the discharge of the vessel. The pressure inside this vessel is kept constant by a pneumatic control device during the whole blowdown experiment (stagnation pressure  $p_0 = 6$  bars). The subcooling of the liquid at the stagnation conditions is varied between 40 and 10°C. The upstream and downstream vessels (catch tank) are linked by a discharge line which consists of the following elements: a ball valve, a vertical pipe, a manual control valve, the horizontal test section and a catch tank connected to the atmosphere. The pressure in the catch tank (back-pressure) can be controlled by filling it initially with compressed air and adjusting the valve located on the exhaust pipe connected to the atmosphere.

Two geometrical configurations of the test section are studied:

- a circular orifice of diameter  $D_{\text{orif}}$  equal to 0.017 or 0.020 m inside a horizontal pipe of diameter  $D$  equal to 0.0284 m. The total pipe length  $L$  is 2.8 m. The cross-sectional area ratio of the orifice  $\mu = (D_{\text{orif}}/D)^2$  is 0.358 or 0.496. The singularity is located at the middle of the relief line;
- an abrupt enlargement with an upstream pipe diameter  $D_{\text{up}}$  of 0.017 m and length  $L_{\text{up}}$  of 1.4

m, and a downstream pipe diameter  $D_{\text{down}}$  of 0.0284 m and length  $L_{\text{down}}$  of 1.4 m. The cross-sectional area ratio of the abrupt enlargement  $\sigma = (D_{\text{up}}/D_{\text{down}})^2$  is 0.358.

The test section tubes are made in Pyrex glass in order to visualize the flow patterns at the vicinity of the abrupt cross-sectional area change.

The location of the instrumentation is shown in Fig. 2 for the enlargement test section. The same locations have been considered for the orifice test sections. The mass flowrate is measured by means of an electromagnetic flowmeter located at the bottom of the vertical pipe. The limiting values of the water characteristics in the upstream vessel (6 bars and 150°C) are related to this flowmeter: temperature cannot exceed 150°C and the fluid is necessarily a liquid. The temperature is measured by chromel–alumel thermocouples at five locations (three thermocouples are located on the test section, one upstream from the manual valve and one in the catch tank). Pressure measurements are made in 19 locations along the horizontal part of the relief line. A double optical probe (BS1, Fig. 2) located just downstream from the singularity (2 mm from the outlet of the upstream pipe) gives measurements of the local void fraction (i.e. the local volumetric fraction of vapour) as well as the axial bubble velocity at the flow axis (Miller and Mitchie, 1969). A data acquisition system enables the recording and the observation of the instantaneous values of the physical variables on a PC during the experiment itself.

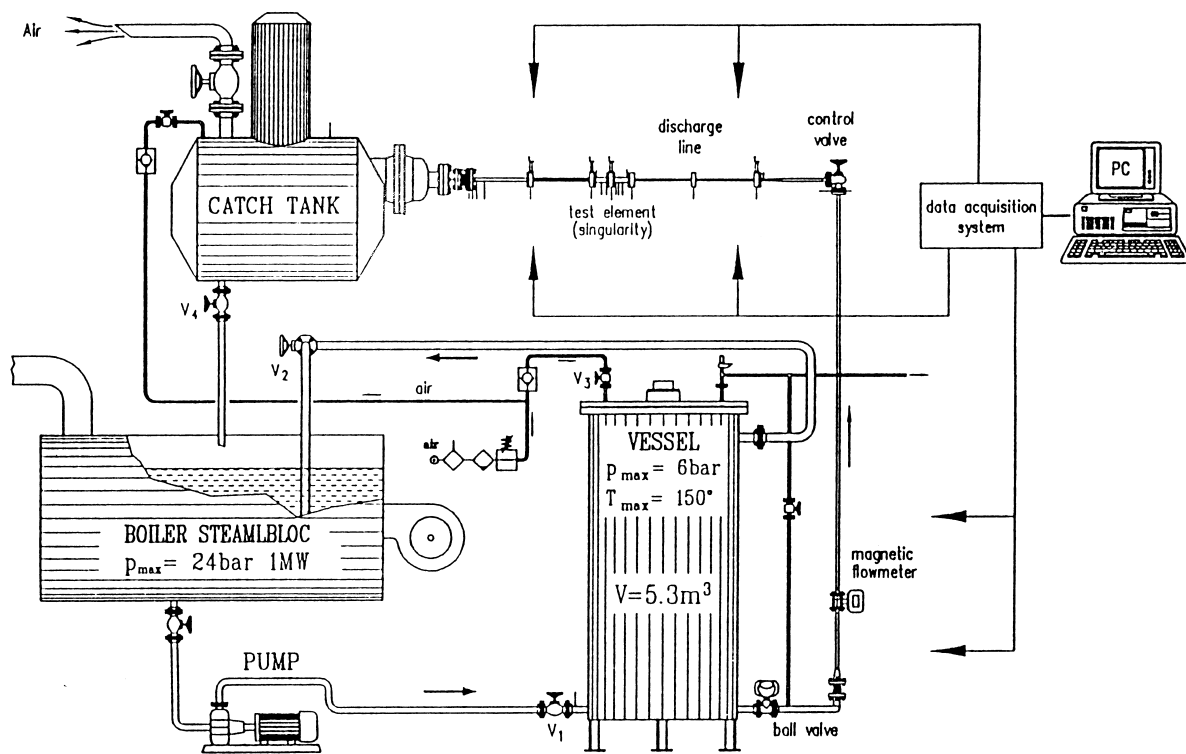


Fig. 1. Sketch of the experimental test facility.

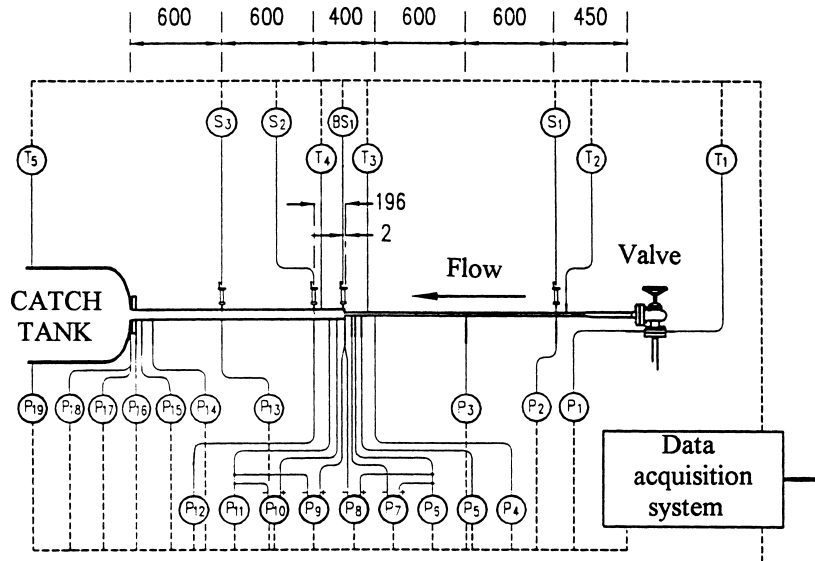


Fig. 2. Instrumentation of the test section.

The experimental procedure for one test is described as follows:

- (a) the value of the back-pressure  $p_r$ , equal to the pressure in the upstream vessel at the beginning of the blowdown, is slowly reduced until the atmospheric pressure is reached ( $p_r$  varies between 6 and 1 bar). This first step of the experiment shows clearly the occurrence of critical conditions.
- (b) for a value of the back-pressure  $p_r$  equal to the atmospheric pressure  $p_{atm}$ , the manual valve upstream from the test section is progressively closed to adjust the pressure at the entrance  $p_e$  to various desired values ( $p_e$  varies between 5 and 1.5 bars). This second step of the experiment generates various inlet conditions of the choked flow.

The subcooling of the liquid at the entrance  $\Delta T_{sat,e}$  is varied between 0 and 14°C. For some tests performed with the test section involving the abrupt enlargement, conditions of two-phase mixture are generated at the inlet of the relief line. For these tests, the quality  $x_e$  is varied

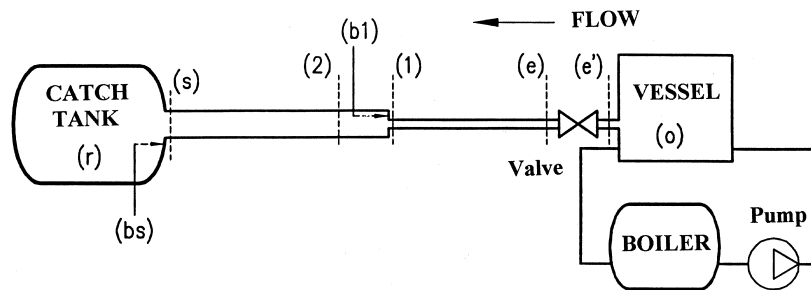


Fig. 3. Notations related to the test section.

between 0 and 0.06. The notations related to the relief line involving the sudden enlargement are indicated in Fig. 3:

- 0 stagnation conditions in the upstream vessel
- e inlet of the relief line
- l outlet of the upstream pipe
- bl separated flow region in the vicinity of the step of the abrupt area change
- s outlet of the relief line
- bs separated flow region surrounding the central jet emerging from the exit of the relief line
- r conditions in the catch tank

The same notations are used for the relief line involving an orifice.

### 3. Flashing jet flow patterns

The phenomenological description of two-phase flashing flow at the vicinity of a geometrical singularity is not much treated in the literature. It is interesting to analyse the structure of the flashing jet emerging from an abrupt area change and the associated transfer phenomena in order to support the interpretations of some characteristics of the critical flow as the location of the critical section, critical mass flowrate and pressure ratio, etc. Some results of visualisations obtained for the enlargement test section are presented below. Similar patterns have been observed for the two-phase flashing flow at the vicinity of the orifice.

#### 3.1. Fluid largely subcooled at the inlet

The picture presented in Fig. 4 is obtained for an inlet temperature of  $T_e = 120.8^\circ\text{C}$  and for an inlet pressure of  $p_e = 2.96$  bars. The back-pressure is close to the atmospheric pressure ( $p_r = 1.35$  bar) and the flow is choked ( $Q_d = 11.12$  m<sup>3</sup>/h). The fluid is largely subcooled at the inlet ( $\Delta T_{\text{sat},e} = 12.3^\circ\text{C}$ ) and the flashing inception occurs at the vicinity of the enlargement. It can be seen that the streamlines of the central flow at the vicinity of the enlargement remain quasi parallel to the pipe axis. The reattachment point is located well beyond the singularity in agreement with measurements of the distance of maximum pressure (Attou and Bolle, 1996). This confined free jet pattern is axisymmetric and the central flow appears to be conical with a small opening angle.

The annular zone surrounding the jet is not occupied by vapour only. In fact, a still liquid layer can be observed at the bottom of the duct near the step. The depth of this liquid layer decreases progressively and vanishes far upstream the reattachment point. Due to the thermal non-equilibrium delay of the liquid phase, the central zone of the flow remains at the superheated liquid state. That causes a radial heat transfer and boiling is confined at the jet boundary. Indeed a high density of small bubbles has been observed at the jet boundary layer. Generated vapour is submitted to condensation through contact with the wall pipe. The film of condensate flows into the bottom by gravity. This process as well as the deposition of droplets contribute to feed the static liquid layer. On the other hand, the boundary layer of static liquid

is submitted to the vaporisation due to the vapour convection. At equilibrium, the two antagonist processes compensate.

The confined jet pattern is not influenced by the back-pressure, the base pressure  $p_{bl}$  (i.e. the pressure existing in the separated flow region in the vicinity of the step) remaining approximately equal to the mean pressure just upstream from the enlargement (for the test presented in Fig. 4,  $p_{bl} = 1.973 \text{ bars} \approx p_{Cl} = 2.001 \text{ bars}$ ).

### 3.2. Liquid close to the saturation at the inlet

The picture presented in Fig. 5 is obtained for an inlet temperature of  $T_e = 150.5^\circ\text{C}$  and for an inlet pressure of  $p_e = 4.96 \text{ bars}$ . The back-pressure is close to the atmospheric pressure ( $p_r = 1.35 \text{ bar}$ ) and the flow is choked ( $Q_d = 5.965 \text{ m}^3/\text{h}$ ). The liquid is close to the saturation at the inlet ( $\Delta T_{\text{sat},e} = 1.1^\circ\text{C}$ ) and the flashing inception occurs close to the inlet of the line. It can be seen that the streamlines of the central flow at the vicinity of the enlargement diverge strongly from the pipe axis. The separated zone does not exist practically. The reattachment point is located at a very small distance from the singularity in agreement with measurements of the distance of maximum pressure (Attou and Bolle, 1996). This expanded jet pattern is not exactly symmetrical around the axis due to the interaction of the jet boundary with the static liquid at the bottom of the pipe. This interaction induces a heterogeneous distribution of the shear stress on the jet boundary. The expanded jet pattern depends on the back-pressure. In

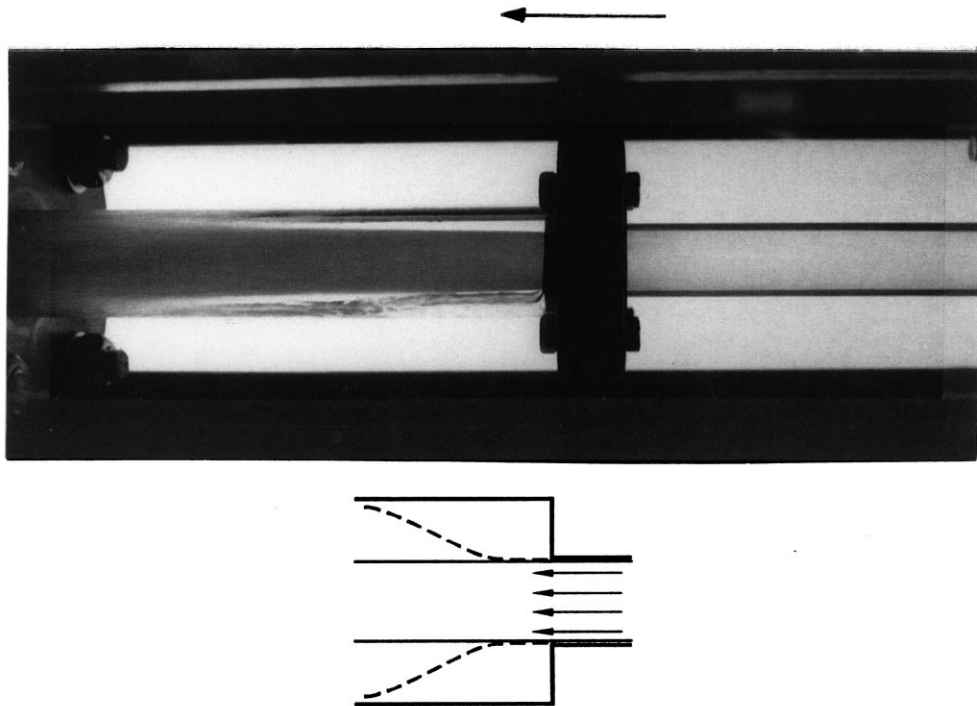


Fig. 4. Confined quasi free jet pattern.

fact, the decrease of the back-pressure leads to a decrease of the base pressure  $p_{bl}$ , and in consequence, the two-dimensional effects at the vicinity of the enlargement become more significant (for the test presented in Fig. 5,  $p_{bl} = 3.143 \text{ bars} < p_{Cl} = 3.886 \text{ bars}$ ).

### 3.3. Two-phase mixture at the inlet

The picture presented in Fig. 6 is obtained for an inlet quality of  $x_e = 2.03 \times 10^{-2}$  and for an inlet pressure of  $p_e = 2.07 \text{ bars}$ . The back-pressure is close to the atmospheric pressure ( $p_r = 1.06 \text{ bar}$ ) and the flow is not choked ( $Q_d = 1.36 \text{ m}^3/\text{h}$ ). In these conditions of two-phase flow at the inlet, the reattachment point begins to move downstream from the enlargement when the inlet quality  $x_e$  increases. The two-dimensional effects become less significant compared to the case of expanded jet pattern. This submerged jet pattern is illustrated in the picture of Fig. 6. The composition of the separated zone is close to the central flow one. This structure is similar to the one observed for the subcritical incompressible flow.

## 4. Experimental evidence of the double-choked flow phenomenon or the two simultaneous locations of critical sections

The experimental facility described above is able to generate flows with various values of the

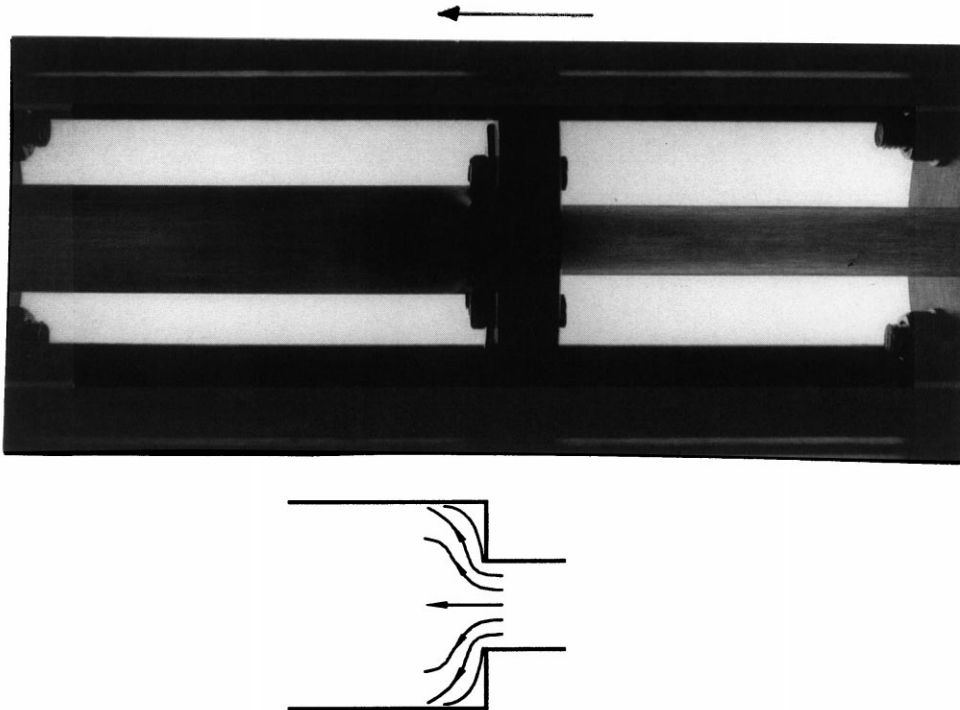


Fig. 5. Expanded jet pattern.



back-pressure  $p_r$ . That allows to explore several flow regimes. At the beginning of a test, the back-pressure is close to the pressure in the upstream vessel. The decrease of back-pressure during the period of a discharge has been kept slow enough to stay all the time as close as possible to the steady-state flow regime.

The analysis of the results shows that the initial subcooling of the fluid  $\Delta T_{\text{sat},0}$  has an important influence in the behaviour of the flow variables during the decrease of the back-pressure, particularly close to the abrupt area change. Accordingly, for each test section, the results are presented for the two extreme investigated values of the stagnation subcooling  $\Delta T_{\text{sat},0}$ .

#### 4.1. Results for the abrupt enlargement test section

##### 4.1.1. Condition of high stagnation subcooling

The evolution of the measured parameters in the case of a high stagnation subcooling ( $\Delta T_{\text{sat},0} = 40.5^\circ\text{C}$ ) during the slow decrease of the back-pressure is reported in Figs. 7–9. Three different flow regimes can be observed.

4.1.1.1. *Single-phase liquid flow (for time < time (A), see Fig. 8).* In the early stage of the blowdown (high values of the pressure ratio  $p_r/p_0$ ), the pressure at any cross-section along the relief line is higher than the saturation pressure corresponding to the local temperature. The

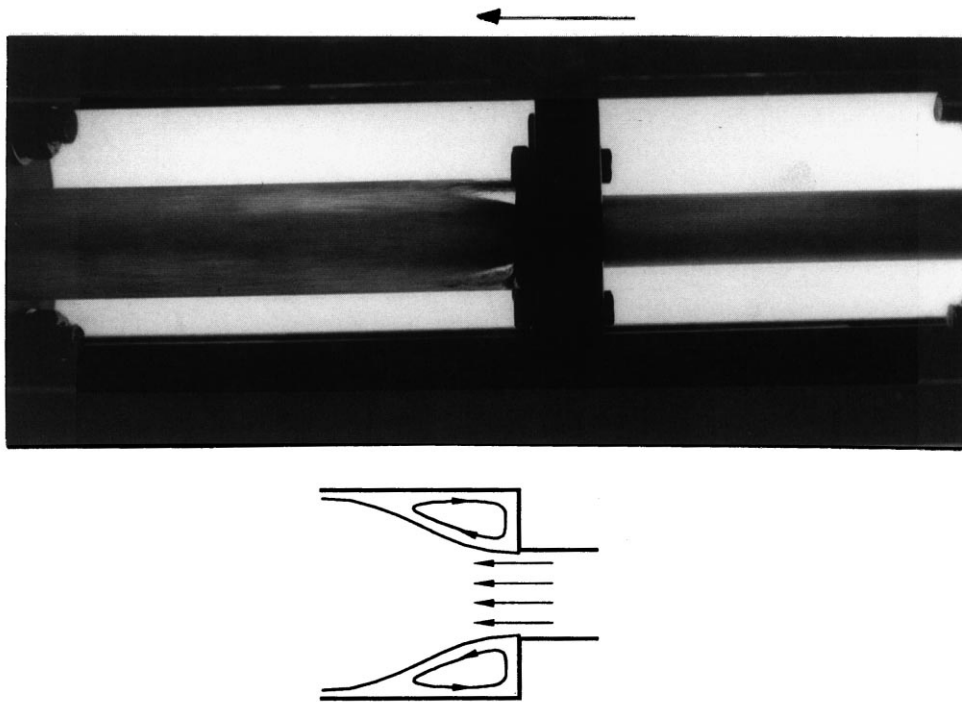


Fig. 6. Submerged jet pattern.

void fractions measured at the pipe axis just downstream from the enlargement ( $\alpha_{1,0}$ ) and at a distance of  $7 D_2$  after the singularity ( $\alpha_{2,0}$ ) remain equal to zero (Fig. 8). In this range of back-pressure, a single-phase liquid flow occurs. The pressure profile presents three zones: a linear decrease of pressure upstream from the enlargement due to the wall friction, a zone of non-linear pressure recovery downstream from the enlargement due to the deceleration of the fluid and a linear decrease of pressure due to the fully established wall frictional shear stress along the downstream duct (Fig. 9). On the other hand, the decrease of the back-pressure induces a monotonous non-linear increase in mass flowrate that remains limited by the hydraulic resistance between the two ends of the relief line:

$$\Delta p = p_0 - p_r \sim f \frac{G^2}{2\rho_L}$$

where  $f$  is the friction factor,  $G$  the mass velocity and  $\rho_L$  the liquid density.

Accordingly, the single-phase liquid flow remains in the subcritical regime. The parameter defined by  $\eta_1 = (p_1 - p_{bl})/p_0$ , which represents the degree of radial non-uniformity of the pressure at the abrupt enlargement, is less than 0.4–0.5% indicating that the pressure is uniform across the cross-section of the pipe located just downstream from the enlargement. The other parameter defined by  $\eta_s = (p_s - p_{bs})/p_0$ , which represents the degree of radial non-uniformity of the pressure at the second enlargement located at the outlet of the line, is also

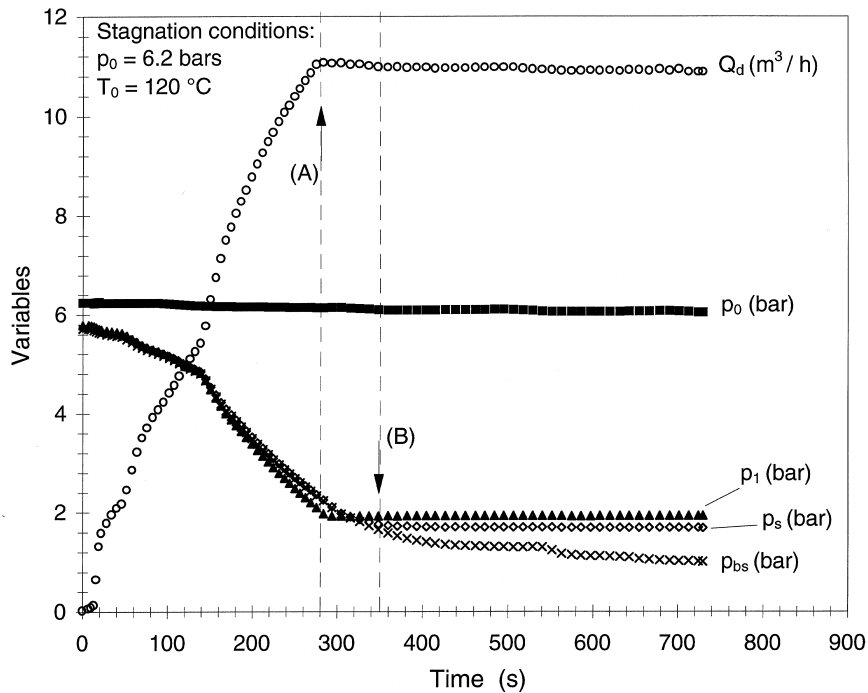


Fig. 7. Evolution of the flow variables during the decrease of the back-pressure: sudden enlargement, high stagnation subcooling  $\Delta T_{\text{sat},0} = 40.5^\circ\text{C}$ .

negligible. The minimum pressure is reached in the flow just downstream from the step enlargement.

4.1.1.2. *Flashing inception and choked flow occurrence (for time (A) < time < time (B), see Fig. 8).* When the pressure ratio  $p_r/p_0$  is further decreased, the minimum pressure on the line becomes less than the saturation pressure corresponding to the inlet temperature. The nucleation process begins in a zone of the central flow downstream from the enlargement. The void fractions in the flow axis,  $\alpha_{1,0}$  and  $\alpha_{2,0}$ , increase quickly (Fig. 8). The established value of the void fraction  $\alpha_{2,0}$  (about 0.75) is much greater than the established value of the void fraction  $\alpha_{1,0}$  (about 0.01) due to essentially two reasons:

- The most probable nucleation process upstream from the step being based on the wall cavity activation (heterogeneous nucleation), the central zone of the flow emerging from the enlargement remains quasi liquid and in a metastable state. That explains the small value of the void fraction  $\alpha_{1,0}$ .
- After the rupture of the free jet, the strong mixing effect caused by the sudden enlargement of the jet and the turbulence induced by the massive vaporisation (homogeneous nucleation) contribute to the relaxation towards the thermodynamic equilibrium conditions. That explains the high value of the void fraction  $\alpha_{2,0}$ .

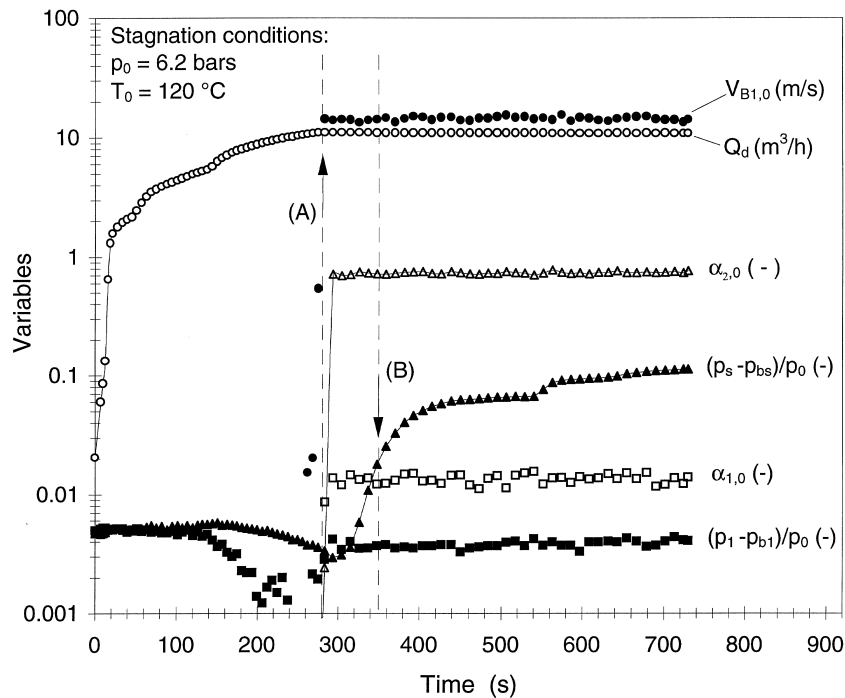


Fig. 8. Evolution of the void fraction and the bubble axial velocity during the decrease of the back-pressure: sudden enlargement, high stagnation subcooling  $\Delta T_{sat,0} = 40.5^\circ\text{C}$ . (A) Occurrence of the first critical section in a region close to the abrupt enlargement and (B) occurrence of the second critical section at the exit of the relief line.

When the void fractions  $\alpha_{1,0}$  and  $\alpha_{2,0}$  become constant, the mass flowrate reaches its maximum possible value which corresponds to the inlet conditions and the geometry of the line located upstream from the critical cross-section. An ulterior decrease of the back-pressure does not change the mass flowrate any more; the flow is choked. The remarkable stability of the mass flowrate is attributed to the stability of the stagnation conditions (pressure and temperature) during the discharge of the vessel. Particularly, the stagnation pressure  $p_0$  is maintained well constant (Fig. 7).

After the occurrence of the choking phenomenon, the pressure  $p_1$  and the mean values of void fractions and axial bubble velocity are not influenced by the back-pressure any more. However, the pressure  $p_s$  at the outlet of the line continues to decrease with the back-pressure (Fig. 7). The measured value of the local axial bubble velocity (about 14–15 m/s) is closed to the volumetric velocity of the mixture evaluated from the measured critical mass flowrate and the pipe cross-sectional area  $A_1$  ( $Q_d/A_1 \cong 13$  m/s). One can think that the correlation technique applied to the double optical sensor signal can be used to evaluate reasonably the local vapour velocity.

From the results obtained for the pressure profile (Fig. 9), four zones can be distinguished:

- in a zone sufficiently upstream from the enlargement, the pressure decreases linearly due to the wall frictional shear stress of the fully established single-phase liquid flow;
- in the vicinity of the upstream pipe outlet, the pressure decreases strongly due to the compressibility effects of the mixture and the fluid acceleration produced by the flashing;
- in a large zone downstream from the enlargement, the pressure remains quasi constant. That

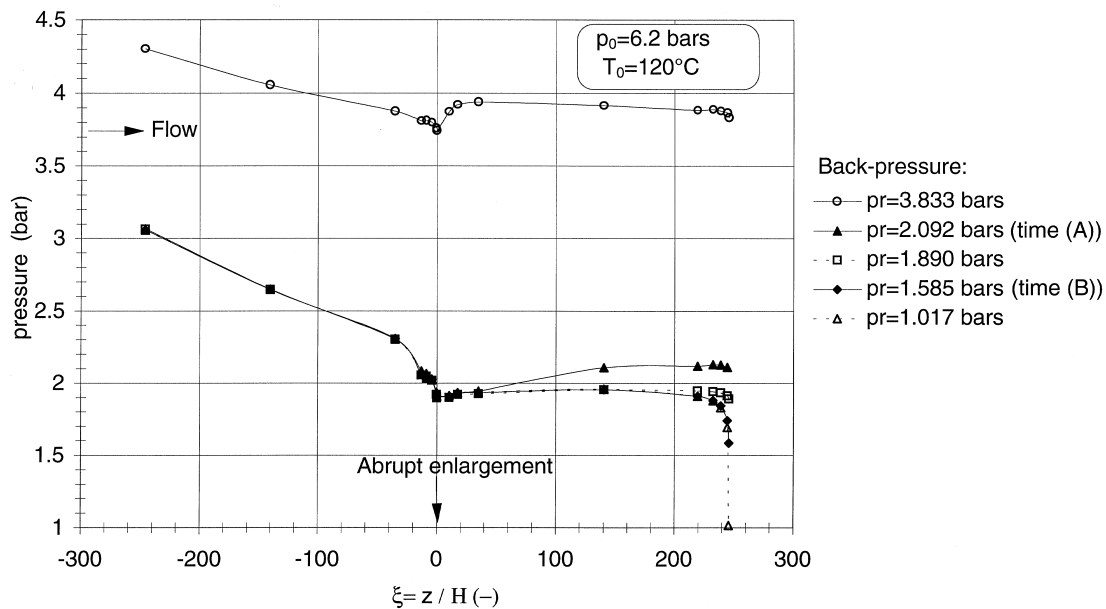


Fig. 9. Evolution of the pressure profile during the decrease of the back-pressure: sudden enlargement, high stagnation subcooling  $\Delta T_{\text{sat},0} = 40.5^\circ\text{C}$ .  $\xi$  is the dimensionless axial distance defined by  $z/H$  where  $H$  is the step height of the enlargement ( $= (D_2 - D_1)/2$ ) and  $z$  is the distance from the abrupt enlargement.

corresponds to the confined free jet pattern characterized by a quasi constant cross-sectional flow area. The pressure in this zone is not influenced by the back-pressure. This means that the critical section is located far away downstream from the singularity. It was difficult to determine accurately the location of critical section due to the limited number of pressure transducers and the small value of pressure gradient. The maximum pressure reached after the jet rupture remains close to the pressure  $p_1$  due to the flow expansion induced by the flashing process;

- close to the outlet of the line, the pressure of the established frictional flow decreases with a gradient depending on the back-pressure.

The parameter  $\eta_1$  remains small with regard to 1 when the flow becomes critical (Fig. 8). That means that the flow region located just downstream from the enlargement behaves as a subcritical zone. This result confirms that the critical section is located in the central zone far away downstream from the upstream pipe exit. Indeed, a high initially subcooling liquid exhibits a significant vaporisation delay due to the non-equilibrium effects. So the jet pattern emerging from the enlargement involves a highly superheated liquid core and, as a consequence, a small void fraction. The critical section is located at the location where the mean void fraction is high enough to cause a severe decrease of the local sound velocity. This location is thus moved downstream from the enlargement when the inlet liquid subcooling decreases.

At the jet outlet far from the enlargement, the residence time of the superheated liquid becomes important enough to produce a massive nucleation. The jet breaks to big droplets separated by rich vapour zones. The homogeneous mixture of big droplets and vapour has been noted by the visual observation and from the optical probe signals detected at  $7 D_2$  from the enlargement. The mixture expands downstream from the critical section to adhere at the pipe wall. The critical flow pattern depends on the mean flow velocity and mean void fraction near the singularity. However, there is any dependence of this structure on the back-pressure because the critical section is located far from the enlargement.

In the early stage of the critical flow occurrence, the measured pressure profile shows that the pressure downstream from the critical section decreases in a monotonous manner up to the value of the back-pressure (Fig. 9). The outlet pressure  $p_s$  decreases with the back-pressure and the pressure profile downstream from the critical section becomes more abrupt. This produces acceleration effects that become very important in a region close to the downstream pipe outlet.

*4.1.1.3. So-called double-choked flow occurrence (for time > time (B), see Fig. 8).* When an enough small value of the ratio  $p_r/p_0$  is reached, the outlet pressure  $p_s$  becomes independent from the back-pressure. The outlet base pressure  $p_{bs}$  (i.e. the pressure existing in the separated flow region surrounding the central jet emerging from the exit of the line) and the outlet pressure  $p_s$  become uncoupled; the parameter  $\eta_s$  begins to increase and it is no longer negligible with regard to one (Fig. 8). The pressure profile does not change any more even if the back-pressure is still decreasing (Fig. 9). This fact shows that the critical conditions are also reached at the outlet of the line. This phenomenon can be physically explained as follows. The averaged flow velocity decreases downstream from the first critical section after the flow again adheres at the

pipe wall. So, the flow becomes subcritical. After establishment of the wall shear stress, the flow through the downstream pipe becomes of the Fanno type, i.e. the adiabatic flow of a compressible fluid through a duct with constant cross-section area (Houberechts, 1976). Accordingly, for a small enough value of the back-pressure, the Fanno effects along the downstream pipe are able to produce a strong acceleration of the fluid up to reach again the local velocity of sound at the exit of the relief line.

This basic experiment clearly shows the occurrence of two simultaneous stable locations of critical sections for a steady-state two-phase flashing flow. It is important to remark that the occurrence of the second critical section does not influence the maximum value of the mass flowrate. This latter is only determined by the first critical cross-section. Thus, in general, there is no one-to-one relationship between the occurrence of a critical section and the maximum mass flowrate concept. But, the occurrence of critical conditions can always be linked with the concept of small pressure disturbances.

It is evident that the double-choked flow phenomenon can only occur when critical conditions can be reached to the vicinity of the abrupt enlargement. This last fact depends essentially on the head frictional loss coefficient ( $\lambda L/D$ ) of the downstream pipe. Indeed, for a high enough value of the head loss coefficient of the downstream pipe, the averaged velocity of the flow becomes equal to the local sound velocity at the line exit due to the Fanno effects. This situation corresponds to the Fanno limit well known in gas dynamics (Houberechts, 1976). This particular value of the head loss parameter is the maximum value  $(\lambda L/D)_{\max}$  which is physically possible. For a value of the ratio  $(\lambda L/D)_{\text{down}}$  greater than this limit  $(\lambda L/D)_{\max}$ , the pressure loss through the downstream pipe corresponds to an entropy production that the fluid cannot overcome. Accordingly, in these conditions, the occurrence of choking conditions at the abrupt enlargement becomes impossible but the flow can be choked at the outlet of the relief line for a small enough value of the back-pressure. This last situation corresponds to a smaller value of the maximum mass flowrate due to the higher frictional dissipation along the whole relief line. As a consequence, the head loss coefficient of the downstream pipe has an influence on the location of the first critical section which has in turn a crucial influence on the maximum mass flowrate.

The limit value of the loss coefficient  $(\lambda L/D)_{\max}$  depends essentially on the cross-sectional area ratio of the enlargement and void fraction at the first critical section (Attou and Seynhaeve, 1998). Although an analytical expression of the maximum head loss coefficient can be found for the ideal gas flow, a similar formula is impossible to obtain for the flashing flow due to the higher complexity of the non linear two-phase flow model. The relatively small downstream pipe length of our test section allows us to highlight the double-choked flow phenomenon even for small pressure difference between the upstream and downstream vessels.

#### 4.1.2. Condition of low stagnation subcooling

The evolution of the same flow parameters in the case of a small stagnation subcooling ( $\Delta T_{\text{sat},0} = 15^\circ\text{C}$ ) is represented in Figs. 10–12. The general observations are similar to the ones discussed in the case of a high stagnation subcooling. When the flow becomes critical, the void fractions are greater and the maximum mass flowrate is smaller compared to the case of high stagnation subcooling conditions. In fact, the nucleation starts close to the inlet of the line and the two-phase length in the upstream pipe becomes more significant in this case.

However, as it can be seen in Fig. 11, the behaviour of some variables are quite different in comparison with the previous case. When the maximum value of the mass flowrate is reached (i.e. critical flow at the vicinity of the abrupt enlargement), the void fractions and bubble velocity continue to increase while the back-pressure is reduced (for time (A) < time < time (B) in Fig. 11). These parameters only become invariant when the double-choked flow situation is reached (for time > time (B) in Fig. 11). Also, the parameter  $\eta_1$  increases and becomes significant when the flow tends to be double-choked. So when the flow becomes critical at the vicinity of the abrupt enlargement, the upstream base pressure  $p_{b1}$  and the pressure  $p_1$  become uncoupled. This shows that the separated zone close to the step enlargement is located downstream from the first critical section. This separated zone remains under the influence of the back-pressure.

For low inlet subcooling conditions, the residence time of the mixture in the two-phase length becomes high enough to produce a relaxation towards the thermodynamic equilibrium conditions in the vicinity of the enlargement. The two-phase jet expands immediately downstream from the enlargement to adhere at pipe wall at a much smaller distance from enlargement than the reattachment distance observed for a high inlet subcooling. Furthermore, one can observe that the maximum pressure is located in a section at a small distance from the enlargement compared to the high inlet subcooling case (Figs. 9 and 12). The fluid emerging from the upstream duct has an expanding jet pattern. The critical section is then located at a very small distance after the exit of the upstream pipe.

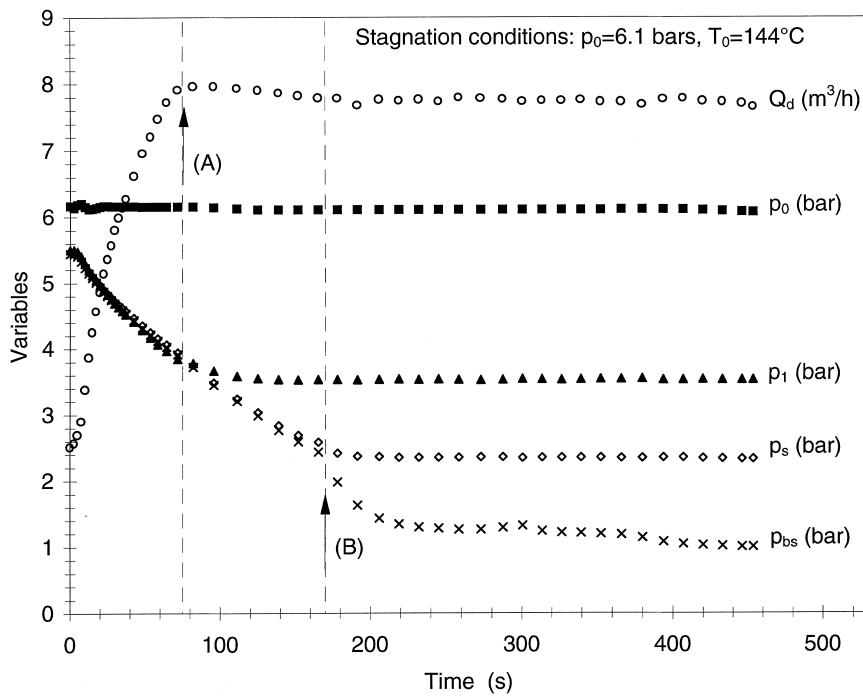


Fig. 10. Evolution of the flow variables during the decrease of the back-pressure: sudden enlargement, small stagnation subcooling  $\Delta T_{sat,0} = 9^\circ\text{C}$ .

#### 4.2. Results for the circular orifice test section

The results obtained with the test section involving a circular orifice essentially show the same phenomenology that one analyzed in test section involving a sudden enlargement. Particularly, the three regimes discussed above are observed. This shows that the multichoking phenomenon is a potentiality of a compressible flow through a discharge line which involves several abrupt changes of the cross-sectional area.

##### 4.2.1. Condition of high stagnation subcooling

The evolution of the measured parameters in the case of a high stagnation subcooling ( $\Delta T_{\text{sat},0} = 40.5^\circ\text{C}$ ) during the slow decrease of the back-pressure is reported in Figs. 13–15.

##### 4.2.2. Condition of small stagnation subcooling

The evolution of the same flow parameters in case of a small stagnation subcooling ( $\Delta T_{\text{sat},0} = 15^\circ\text{C}$ ) is represented in Figs. 16–18.

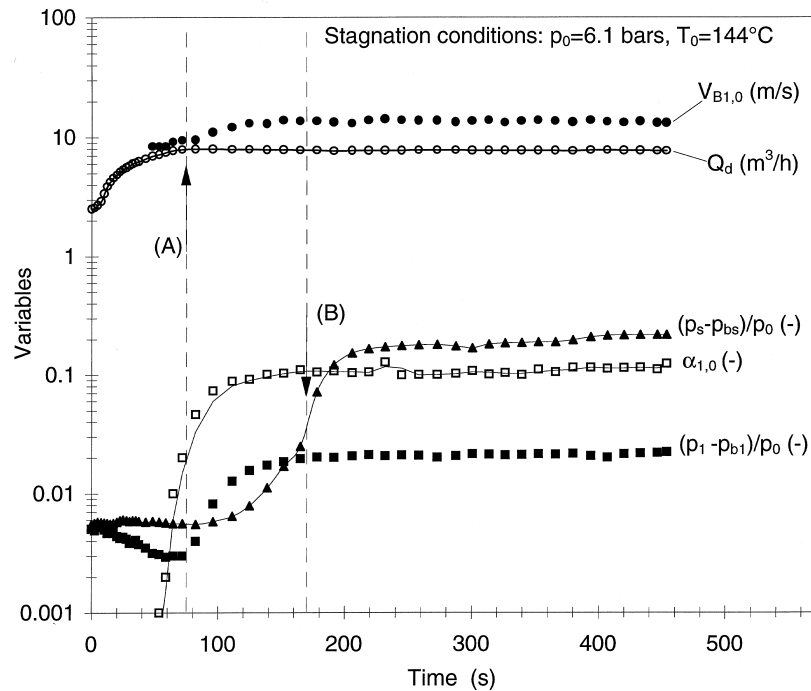


Fig. 11. Evolution of the void fraction and the bubble axial velocity during the decrease of the back-pressure: sudden enlargement, small stagnation subcooling  $\Delta T_{\text{sat},0} = 9^\circ\text{C}$ . (A) Occurrence of the first critical section close to the abrupt enlargement and (B) occurrence of the second critical section at the exit of the relief line.



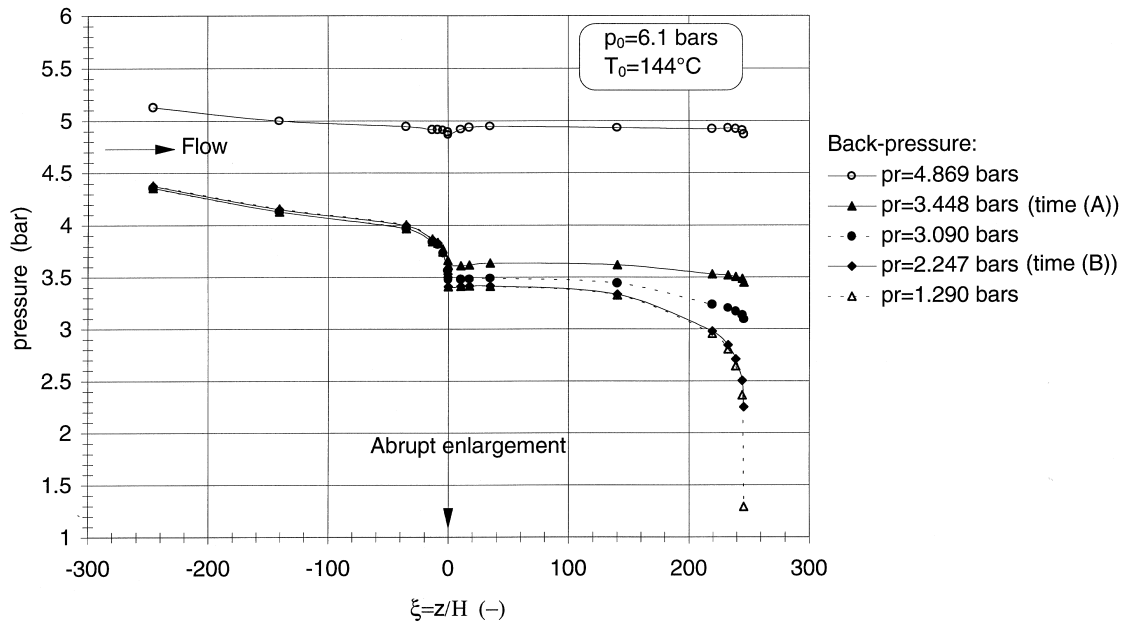


Fig. 12. Evolution of the pressure profile during the decrease of the back-pressure: sudden enlargement, small stagnation subcooling  $\Delta T_{sat,0} = 9^\circ\text{C}$ .

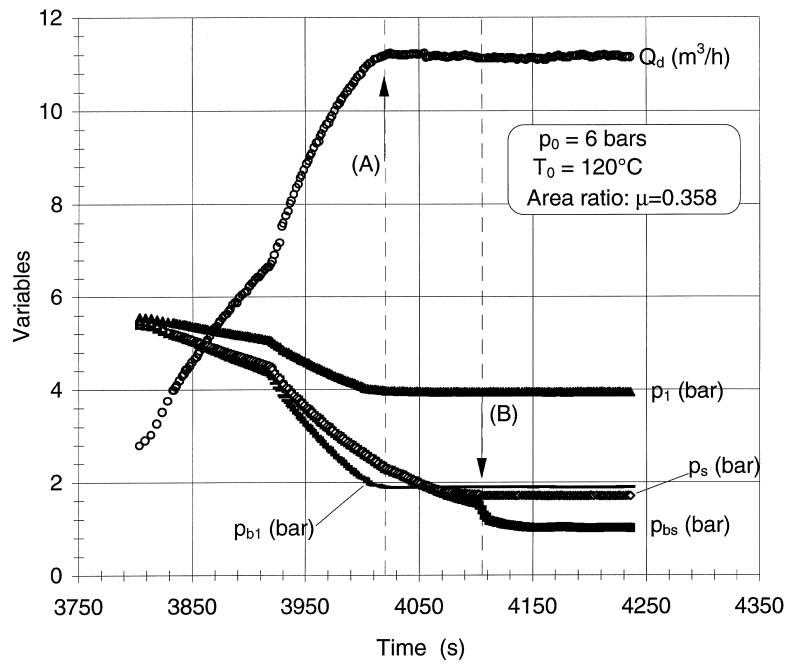


Fig. 13. Evolution of the flow variables during the decrease of the back-pressure: orifice, high stagnation subcooling  $\Delta T_{sat,0} = 40.5^\circ\text{C}$ .

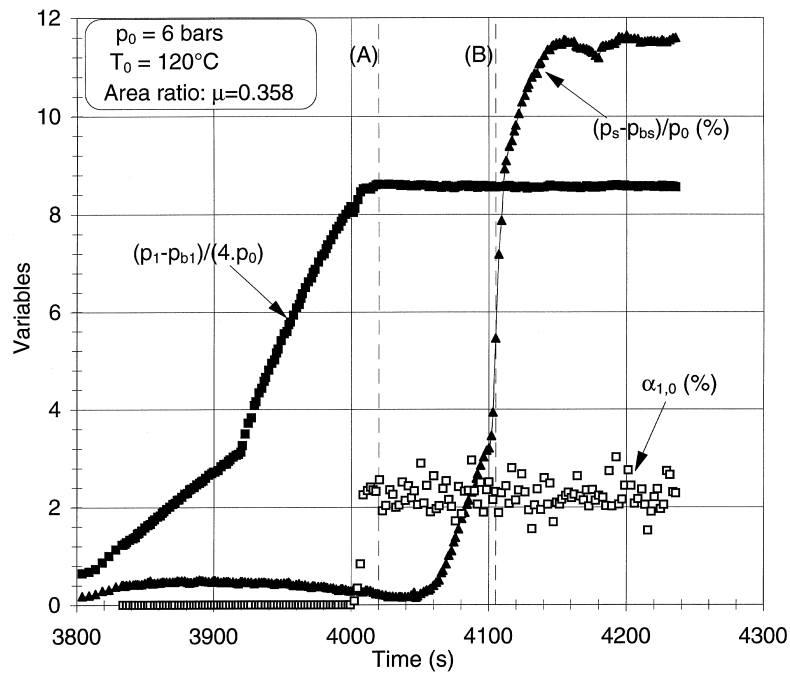


Fig. 14. Evolution of the void fraction and the parameters  $\eta_{pl}$  and  $\eta_{ps}$  during the decrease of the back-pressure: orifice, high stagnation subcooling  $\Delta T_{sat,0} = 40.5^\circ\text{C}$ .

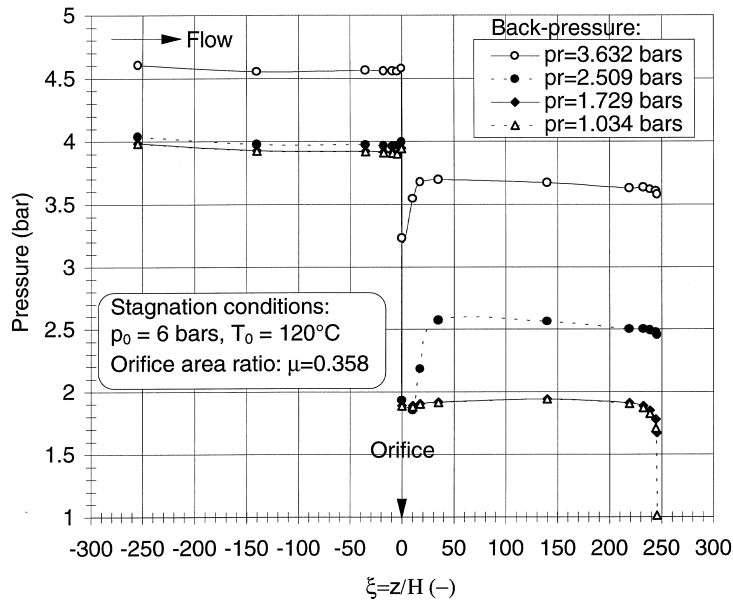


Fig. 15. Evolution of the pressure profile during the decrease of the back-pressure: orifice, high stagnation subcooling  $\Delta T_{sat,0} = 40.5^\circ\text{C}$ .  $\xi$  is the dimensionless axial distance defined by  $z/H$  where  $H$  is the step height of the orifice ( $= (D - D_{orif})/2$ ) and  $z$  is the distance from the orifice.

## 5. Critical mass flowrate and pressure ratio in the relief line involving an abrupt enlargement

### 5.1. Subcooled liquid at the inlet

In the case of the abrupt enlargement, the results of the critical mass velocity (based on the area of the upstream pipe cross-section  $A_1$ ) are plotted in Fig. 19 as a function of the inlet subcooling for several values of the inlet pressure ( $p_e$  between 2 and 5 bars). For all these experiments, the pressure in the catch tank has been kept equal to the atmospheric pressure.

The critical mass velocity increases monotonously with the inlet subcooling. The set of data shows that the critical mass velocity presents a quasi asymptotic behaviour at high subcoolings. This property can be explained on the basis of the flow pattern at the vicinity of the singularity. In fact, for high enough values of the inlet subcooling, the increase in this quantity produces only a little translation of the location of boiling inception inside the jet. Due to the fact that the jet emerging from the enlargement is quasi free (cf. Section 3.1), the necessary pressure drop to induce this translation is small. Accordingly, the pressure in the first critical section, close to the saturated pressure corresponding to the inlet temperature, remains practically invariant ( $p_{Cl} \approx p_{vap}(T_e)$ ). The monotonously increasing behaviour in the case of a long tube has been observed by some authors in the conditions of higher stagnation pressure ( $p_0 = 10\text{--}20$  bars) (Celata et al.,

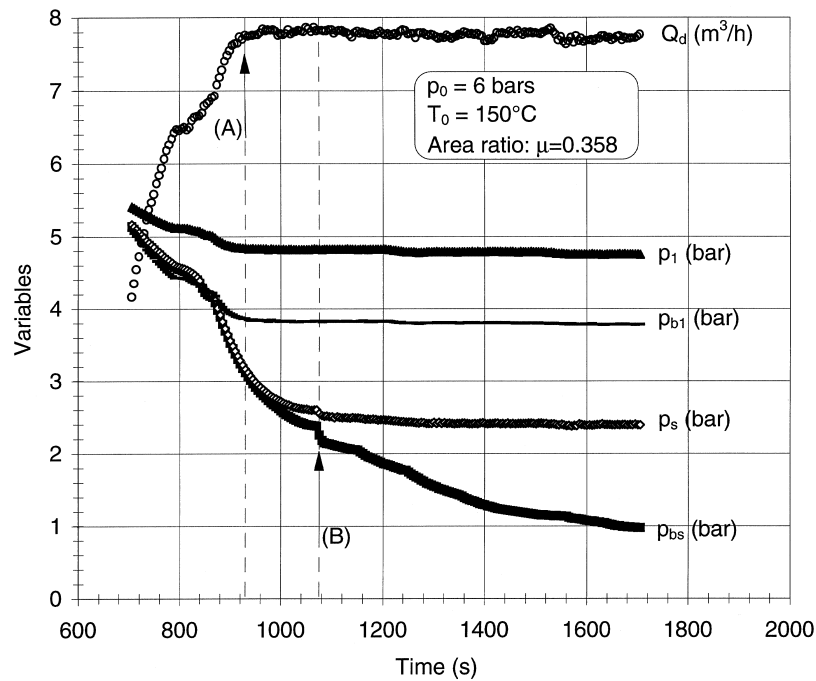


Fig. 16. Evolution of the flow variables during the decrease of the back-pressure: orifice, small stagnation subcooling  $\Delta T_{sat,0} = 9^\circ\text{C}$ .

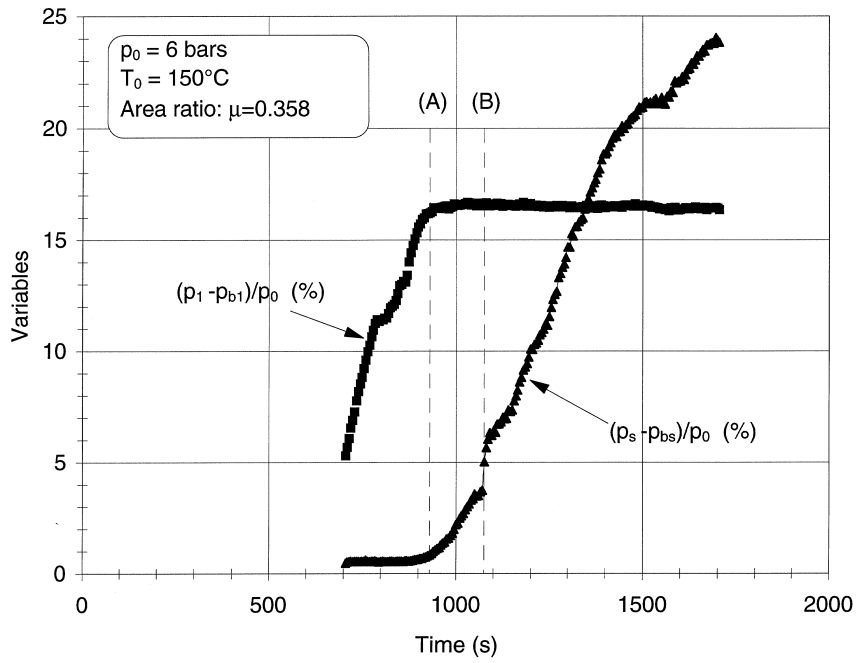


Fig. 17. Evolution of the parameters  $\eta_{pl}$  and  $\eta_{ps}$  during the decrease of the back-pressure: orifice, small stagnation subcooling  $\Delta T_{sat,0} = 9^\circ\text{C}$ .

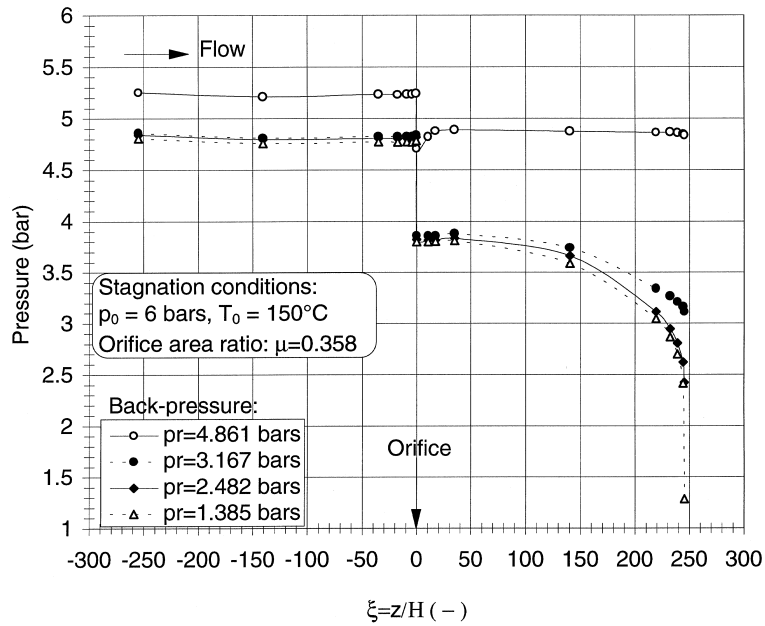


Fig. 18. Evolution of the pressure profile during the decrease of the back-pressure: orifice, small stagnation subcooling  $\Delta T_{sat,0} = 9^\circ\text{C}$ .

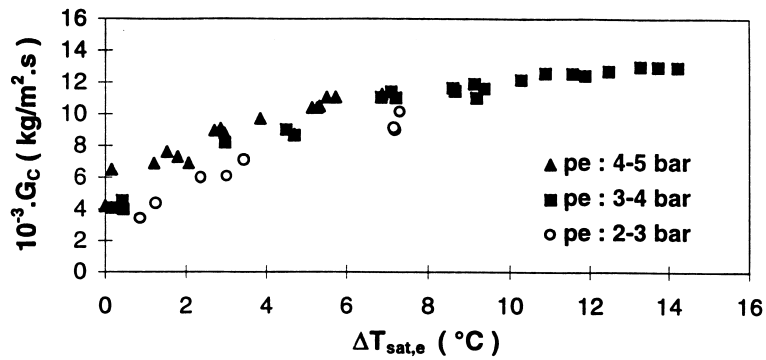


Fig. 19. Critical mass velocity versus the inlet subcooling: sudden enlargement,  $(L/D)_{up} = 82.3$ .

1982). However, the above mentioned asymptotic behaviour has not been identified. A more important influence of the subcooling on the critical mass flowrate has been noted for the safety valve (short pipe geometry; Bolle et al., 1995).

It is important to note that the critical mass velocity measured for high values of the inlet subcooling ( $\Delta T_{sat,e} \approx 12\text{--}14^\circ\text{C}$ ) remains lower than the value corresponding to the liquid flow (for  $T_0 = 35^\circ\text{C}$ ,  $G_1 = 14,230 \text{ kg/m}^2 \text{ s}$ ,  $p_{back} = p_{atm}$ ). Due to the intensive vaporisation produced by the rupture of the liquid jet, the velocity of displacement of small pressure disturbances is indeed dramatically reduced. The influence of the vaporization phenomenon on the mass flowrate characteristic of the relief line is shown in Fig. 20 where the square root of the total pressure drop across the horizontal channel ( $p_e - p_s$ ) is plotted as a function of the mass flowrate. The cooled liquid flow ( $T_0 = 35^\circ\text{C}$ ) is compared with hot water flows ( $T_0 = 140.5$  and  $T_0 = 150.5^\circ\text{C}$ ). For small values of the total pressure drop, the two kinds of characteristic are identical, but for a total pressure drop high enough to produce the inception

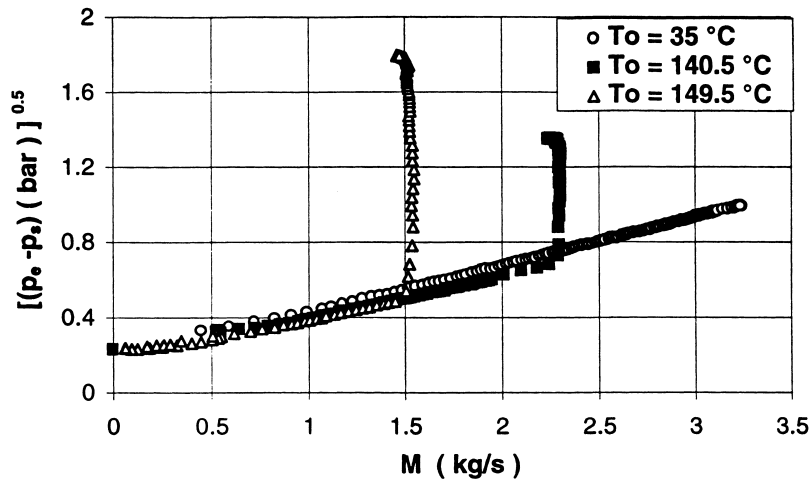


Fig. 20. Influence of the vaporization process on the mass flowrate: sudden enlargement.

of the nucleation process, the two curves begin to diverge; a maximum mass flowrate appears for hot water flashing flows which become critical in a zone downstream from the enlargement, the cold water flow remaining subcritical.

For a given upstream pipe geometry, one can analyse the influence of the pipe geometry downstream from the cross-section  $A_1$  on the critical mass flowrate. For initially high subcooled flow, the streamlines remain, at the cross-section  $A_1$ , parallel to the axis (Fig. 4). The pressure is quasi uniform across this cross-section. The critical section is located far away the step. If the enlargement is replaced by a divergent, for example, the liquid jet remains free. The critical conditions are not much affected since the confined free jet emerging from the cross-sectional area  $A_1$  does not interact intensively with the pipe wall. Accordingly, in these conditions, the downstream pipe geometry has practically no influence on the critical mass flowrate as observed experimentally (Jeandey et al., 1983). For flows initially close to the saturation, the jet is expanding quickly just downstream from the enlargement (Fig. 5). At the cross-sectional area  $A_1$ , the streamlines diverge strongly from the axis due to the lower pressure measured in the separated zone located at the vicinity of the step enlargement. The pressure is thus not uniform across  $A_1$ . The critical section is located just downstream from the enlargement. If this singularity is now replaced by a divergent, for example, the expanded jet becomes more confined by the pipe wall. Accordingly, the two-dimensional effects become less significant at the cross-sectional area  $A_1$  and the physical conditions at the critical section are thus modified. The jet emerging from the upstream pipe is directly submitted to a strong interaction with the pipe wall that depends on the downstream geometry. Accordingly, in these conditions, the downstream pipe geometry has an important influence on the critical mass flowrate as shown experimentally (Henry, 1970).

As in gas dynamics, the critical pressure ratio is defined by  $p_{C1}/p_{e,0}$  where  $p_{e,0}$  is the total pressure at the inlet. The critical pressure ratio versus the inlet subcooling is represented in Fig. 21. The two parameters are well correlated. The non monotonous behaviour of the critical pressure ratio can be explained by the fact that the flow can be subdivided into two parts: the

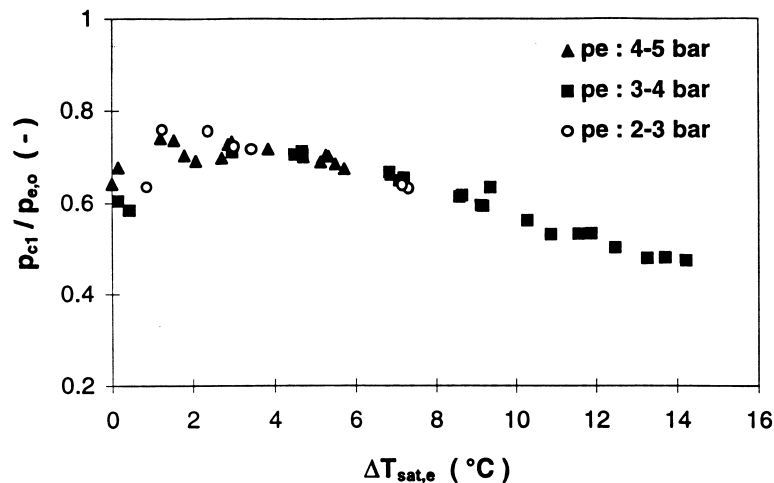


Fig. 21. Critical pressure ratio versus the inlet subcooling: sudden enlargement,  $(L/D)_{up} = 82.3$ .

single-phase zone and the two-phase zone. For high enough inlet subcooling, the flow is quasi liquid all along the upstream pipe up to the saturation at the exit of this pipe. Accordingly, in these conditions, the critical pressure, close to the saturation pressure corresponding to the inlet temperature, is practically unchanged. This constant value corresponds to the one noted previously for the mass flowrate (Fig. 19) in same conditions. Close to saturation conditions at the inlet, the frictional pressure loss and the acceleration pressure drop across the two-phase zone become dominant compared to the ones of the single-phase liquid zone; the critical pressure ratio increases with  $\Delta T_{\text{sat,e}}$ . For intermediary values of the inlet subcooling, the decrease of the mass flowrate corresponds to the decrease of the frictional pressure loss caused essentially by the single-phase zone in spite of the beginning of increase in two-phase zone; the critical pressure ratio decreases when  $\Delta T_{\text{sat,e}}$  increases. The trend shown in Fig. 21 has been also observed by Celata et al. (1982). These authors have shown that this same trend is also independent of the pipe geometry.

### 5.2. Two-phase mixture at the inlet

In the case of the abrupt enlargement, the results of the critical mass velocity (based on the cross-sectional area  $A_1$  of the upstream pipe) are reported in Fig. 22 as a function of the inlet vapour quality (or vapour mass fraction) for various values of the inlet pressure ( $p_e$  between 2 and 4 bars). The critical mass velocity  $G_C$  decreases monotonously with the inlet quality. In the domain of small qualities, the mass velocity  $G_C$  decreases strongly in agreement with the results obtained for the flow of initially saturated liquid through a short or long pipe (Sozzi and Sutherland, 1975). This behaviour is due to the important influence of the two-phase pressure drop (friction and acceleration effects). The influence of the inlet pressure on the critical mass velocity is non negligible, contrary to the observation in the subcooled liquid conditions. On the other hand, for a given upstream geometry, one can analyse the influence of the geometry downstream from the cross-sectional area  $A_1$  on the critical mass flowrate. For two-phase flow at the inlet, the streamlines diverge strongly from the axis at the vicinity of the enlargement, especially for small qualities. The pressure is not uniform across the critical section located

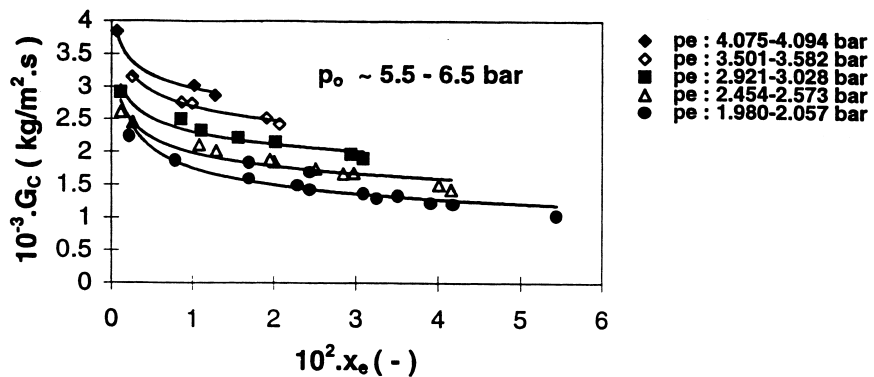


Fig. 22. Critical mass velocity versus the inlet quality: sudden enlargement,  $(L/D)_{\text{up}} = 82.3$ .

close to the step enlargement. A similar phenomenology as for low values of the inlet subcooling is observed. However, when the quality increases, the two-phase jet tends towards a more confined pattern near the enlargement.

The critical pressure ratio  $p_{C1}/p_{e,0}$  versus the inlet quality is represented in Fig. 23. For small values of the inlet quality, the critical pressure ratio decreases quickly when the quality  $x_e$  increases. This confirms the significant influence of the frictional loss and acceleration effects. The pressure ratio is around 0.4–0.5. This agrees with the results obtained by Ogasawara (1969b) for long pipes.

## 6. Critical mass flowrate in the relief line involving a circular orifice

The results of measured critical mass velocity  $G_C$  (based on the cross-sectional area of the pipe) are reported in Fig. 24 as a function of the inlet subcooling. The general trend shows that the critical mass velocity is higher for the orifice of higher diameter  $D_{\text{orif}}$ . In the range of high inlet subcoolings ( $\Delta T_{\text{sat,e}} > 7^\circ\text{C}$ ), the critical mass velocity  $G_C$  can be evaluated with a good approximation by the relation well known in single-phase liquid flow. Indeed, in these conditions, the fluid emerging from the orifice is quasi liquid.

In order to compare the two kinds of geometries, the values of critical mass flowrate of the flashing flow across the orifice or the sudden enlargement of the same cross-sectional area ratio are reported in Fig. 25. One can observe that in the range of high inlet subcoolings ( $\Delta T_{\text{sat,e}} > 7^\circ\text{C}$ ), for which the flow pattern is the same for the two kinds of geometries (confined quasi free jet pattern), a higher value of the mass flowrate is observed in the relief line with the sudden enlargement. This fact is attributed to the existence of a vena contracta just downstream from the orifice as well as the thermal non-equilibrium effects in the liquid phase. In fact, the liquid superheat is much higher in the case of the orifice due to the more important acceleration induced by this singularity compared to the other one. Accordingly, the quality reached in the first critical section is expected to be higher in the case of the orifice. The

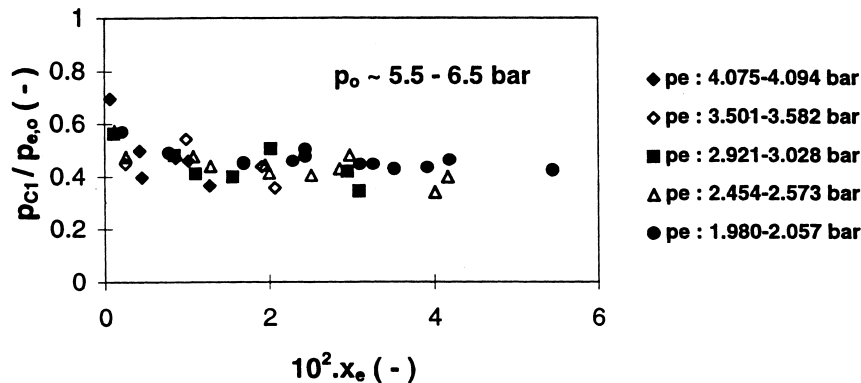


Fig. 23. Critical pressure ratio versus the inlet quality: sudden enlargement,  $(L/D)_{\text{up}} = 82.3$ .



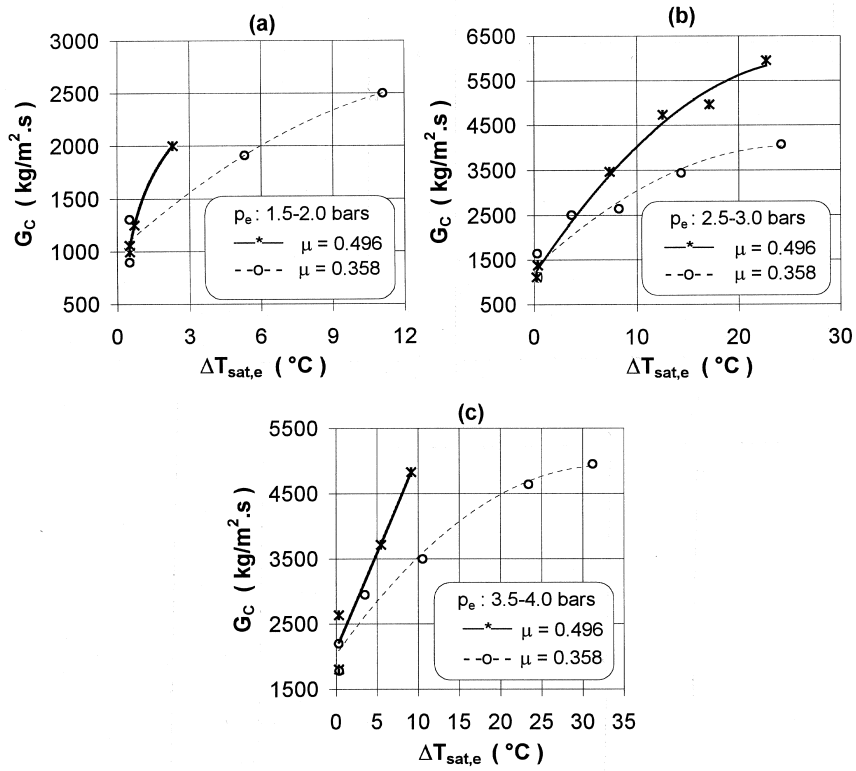


Fig. 24. Critical mass velocity versus the inlet subcooling: orifice.

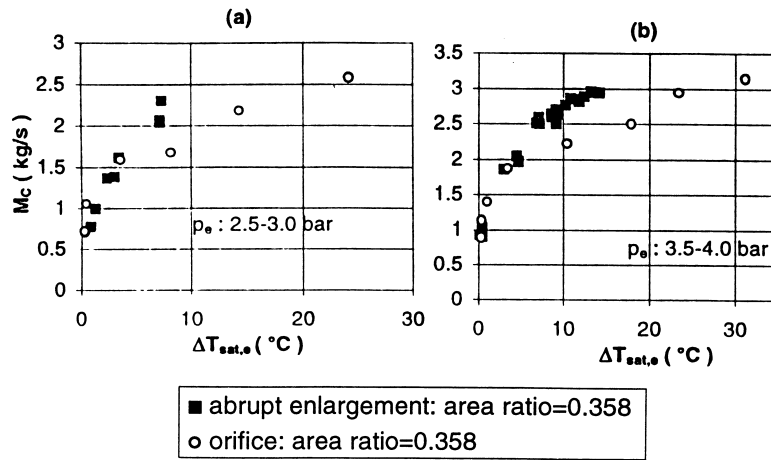


Fig. 25. Comparison of the two kinds of geometries in term of the critical mass flowrate versus the inlet subcooling.

local velocity of sound being dramatically reduced by the quality (in the range of small qualities), a smaller value of the mass flowrate is observed for the orifice.

## 7. Conclusions

New experimental results are obtained for critical steady-state two-phase steam–water flows through a horizontal relief line involving an abrupt cross-sectional area change. Two geometrical singularities have been tested: the sudden enlargement and the circular orifice.

For both singularities, the experimental evidence of the double-choked flow phenomenon has been clearly shown by means of experiments carried out by varying the back-pressure. For a small enough value of the back-pressure, two simultaneous steady-state locations of critical sections are found; one critical section is located close to the abrupt area change and the other is located at the outlet of the relief line. The maximum possible value of the mass flowrate is limited by the first critical section only. The possibility of occurrence of this phenomenon depends on the frictional head loss coefficient of the pipe located downstream from the singularity. A value of this coefficient higher than the one corresponding to the Fanno limit of the flow through the downstream pipe prevents the critical conditions to be reached at the vicinity of the geometrical singularity.

Depending on the inlet conditions, the flow patterns just downstream from the singularity can be quite different. For high subcooling of the liquid at the inlet, a confined free jet pattern is observed over a long distance from the singularity (up to 10 upstream diameters). The first critical section is located just after the rupture of the jet and the critical mass flowrate and pressure ratio do not depend on the downstream pipe geometry. Close to the saturation at the inlet, the jet is expanded quickly up to the wall. The first critical section is very close to the singularity and the critical mass flowrate and pressure ratio are influenced by the downstream pipe geometry. The critical mass flowrate and pressure ratio depend strongly on the inlet conditions. The behaviour of these hydrodynamic parameters is explained on the basis of physical considerations of jet patterns, frictional pressure losses and acceleration effects. It is obvious that the flashing jet flow patterns give a simple explanation of the various phenomena observed in critical flow. Further experimental studies with a more sophisticated instrumentation have to be carried out in order to investigate the local phenomena at a higher level of complexity.

Finally, further experimental work needs to be carried out at much higher pressures with flashing systems involving organic fluids, used in the industrial practice and with pressure relief lines involving several geometrical singularities. These experimental results are still required to validate the design as well as the operation of pressure relief lines, which could exhibit the multichoking phenomenon in the case of high velocity multiphase compressible flows.

## References

- Alimonti, C., 1996. Etude de l'écoulement critique de mélanges polyphasiques dans des scénarios d'accident de relâchement, Thèse de Doctorat en Sciences Appliquées, Université catholique de Louvain, Louvain-la-Neuve.

- Attou, A., Bolle, L. 1996. Analyse d'un écoulement critique en vaporisation à travers une ligne de transport comportant un élargissement brusque. In: Desmet, B., Baudoin, B., Lassue, S. (Eds.), *Thermique et Transports*. Elsevier, Amsterdam, pp. 405–410.
- Attou, A., Bolle, L., Franco, J., Seynhaeve, J.M., 1996. Flow through singularities and ducts downstream of safety valves, Final Report of Environment Program, Contract EV5V-CT93- 0289, CEC, Université catholique de Louvain.
- Attou, A., 1997. Les écoulements diphasiques critiques et subcritiques à travers les singularités / Tomes I et II, Thèse de Doctorat en Sciences Appliquées, Université catholique de Louvain, Louvain-la-Neuve.
- Attou, A., Seynhaeve, J.M., 1998. Computation of steady-state multiple choked compressible flow: an analytical solution for single- and two-phase two-component flow. *J. Loss Prevention in the Process Industries* 11, 229–247.
- Bolle, L., Downar-Zapolski, P., Franco, J., Seynhaeve, J.M., 1995. Flashing water flow through a safety valve. *J. Loss Prevention in the Process Industries* 8, 111–126.
- Celata, G.P., Cumo, M., Farello, G.E., 1982. Critical flows of subcooled liquid and jet forces, Report RT-ING(82)18, ENEA.
- Delhaye, J.M. 1981. Two-phase flow and heat transfer in the power and process industries. In: Bergles, A.E., Collier, J.G., Delhaye, J.M., Hewitt, G.F., Mayinger, F. (Eds.), *Singular Pressure Drops*. Hemisphere, New York, pp. 124–150.
- Fauske, H.K., 1965. The discharge of saturated water through tubes. *Chem. Eng. Prog. Serie* 61 59, 210–216.
- Fletcher, B., Johnson, A.E., 1983. The discharge of superheated liquids from pipes. I. *Chem. E. Symp. Series* 85, 149–156.
- Giot, M. 1981. Thermohydraulics of two-phase systems for industrial design and nuclear engineering. In: Delhaye, J.M., Giot, M., Riethmuller, M.L. (Eds.), *Critical Flows*. McGraw-Hill, New York, pp. 405–452.
- Henry, R.E., 1970. The two-phase critical discharge of initially saturated or subcooled liquid. *Nuclear Science and Engineering* 41 (3), 336–343.
- Henry, R.E., Fauske, H.K., 1971. The two-phase critical flow of one-component mixtures in nozzles, orifices, and short tubes. *J. Heat Transfer* 93 (2), 179–187.
- Houbrechts, 1976. *Thermodynamique technique/Tome II*, Ceuterick, Louvain.
- Hsu, Y.Y., Graham, R.W. 1986. Critical flow rate, propagation of pressure pulse, and sonic velocity in two-phase media. In: *Transport Processes in Boiling and Two-Phase Systems*. American Nuclear Society, IL, pp. 331–368 chapter 11.
- Jandey, Ch., Gros d'Aillon, L., Barrière, G., Bourguine, R., Verdun, C., 1983. Mesure de débits critiques sur l'installation Super Moby Dick dans une section d'essais comportant un divergent ou un élargissement brusque, Private communication, TT/SETRE/82-32, CEA-IRDI, Département des réacteurs à eau, S.E.T.R.E.
- Miller, M., Mitchie, R.E., 1969. The development of an universal probe for measurement of local voidage in liquid–gas two-phase flow. In: *ASME Symposium on Two-Phase Flow Instrumentation*, Chicago, IL, 82–88.
- Morris, S.D., 1990. Flashing flow through relief lines, pipes breaks and cracks. *J. Loss Prevention in the Process Industries* 3, 17–26.
- Ogasawara, H., 1969a. A theoretical approach to two-phase critical flow. 5th Report Bulletin JSME 12 (52), 847–856.
- Ogasawara, H., 1969b. A theoretical approach to two-phase critical flow. 4th Report Bulletin JSME 12 (52), 837–846.
- Schmidt, J., Friedel, L., 1997. Two-phase pressure drop across sudden contractions in duct areas. *Int. J. Multiphase Flow* 23 (2), 283–299.
- Seynhaeve, J.M., 1977. Critical flow through orifices, European Two-Phase Flow Group Meeting, Grenoble.
- Sozzi, G.L., Sutherland, W.A., 1975. Critical flow of saturated and subcooled water at high pressure. In: *ASME Symp. of Non-Equilibrium Two-Phase Flows*, 19–25.
- Tapucu, A., Teyssedou, A., Troche, N., Merilo, M., 1989. Pressure losses caused by area changes in a single-channel flow under two-phase flow conditions. *Int. J. Multiphase Flow* 15 (1), 51–64.
- Van den Akker, H.E.A., Bond, W.M., 1984. Discharges of saturated and superheated liquids from pressure vessels. In: *Symp. on Protection of Exothermic Reactors and Pressurized Storage Vessels*, Chester, UK.
- Zaloudek, F.R., 1963. The critical flow of hot water through short tubes, Report HW-77594/UC38, Hanford Laboratories.